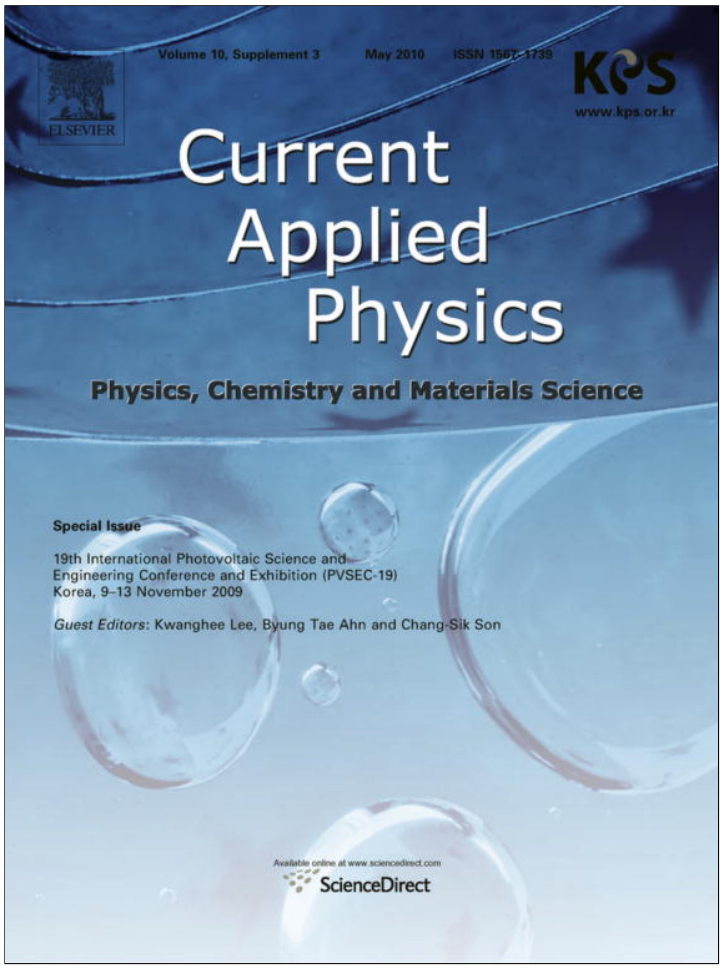

Current Applied Physics 10 (2010) S520–S524

Contents lists available at ScienceDirect

Current Applied Physics

journal homepage: www.elsevier.com/locate/cap

Effects of thermal annealing on the efficiency of bulk-heterojunction organic photovoltaic devices

Jin Wook Jeong [a,c], Jin Woo Huh [a], Jeong Ik Lee [b], Hye Yong Chu [b], Il Ki Han [c], Byeong-Kwon Ju [a,*]

[a] Display and Nanosystem Lab., College of Engineering, Korea University, Seoul 136-713, Republic of Korea
[b] Convergence Components & Materials Research Lab., Electronics and Telecommunications Research Institute, Daejeon 305-350, Republic of Korea
[c] Nano Device Research Center, Korea Institute of Science and Technology, Seoul, Republic of Korea

ARTICLE INFO

Article history:
Received 2 November 2009
Received in revised form 1 February 2010
Accepted 16 February 2010
Available online 21 February 2010

Keywords:
Morphology
Absorption
Organic solar cells
Photovoltaic
Annealing

ABSTRACT

This paper studies the effect of the annealing process on the performance of P3HT/PCBM photovoltaic devices, in terms of their efficiencies. The basic photovoltaic devices are annealed on a hot-plate, at a temperature of 150 °C for 10 min in air. For comparison, the thermal annealing of photovoltaic devices is carried out using rapid thermal annealing (RTA) equipment, at a temperature of 150 °C for 10 min in different environments such as in vacuum, in nitrogen and in argon, individually. The light conversion efficiency (E_{ff}) of the resulting photovoltaic devices increases from 2.29% (hot-plate annealing) to 2.77% after annealing in a vacuum environment. As a result, the organic photovoltaic devices, annealed in a vacuum show enhanced efficiencies compared with those annealed in different gas environments.

1. Introduction

Conjugated polymers have been widely used in organic photodiodes and organic photovoltaic devices based on organic semiconductor materials, because of their advantages, which include the following: they require a simplified fabrication process which is also at low-temperatures, they are low-cost, have good flexibility, high-quantum efficiencies, and high-absorption coefficients [1–3]. The high efficiency photovoltaic devices in particular, based on conjugated polymer and fullerene composites, are key in many important applications such as wearable displays, radio frequency (RF) identification tags and smart cards [4,5]. Flexible batteries and photovoltaic devices might also be possible candidates for this type of application. Thus, because of these practical advantages, previous research topics have focused on high efficiency [6,7], wide band gap [8,9], large area processing [10,11], stability [12,13], free transparent electrodes [14,15] and others [16,17]. However, organic photovoltaic device performances are generally poor in comparison with photovoltaic devices based on III–V compounds or silicon [18], but recent studies have reported remarkably improved performances of the these photovoltaic devices, by up to 5% in a single device structure, through studies such as varying the ratio of donor–acceptor materials [19,20], optimizing the annealing time and the annealing temperature of the active layer [21,22], the type of electrical treatment used [23,24], the type of adhesive layer on or under the anode or cathode layer [25,26], and using various active materials having a wide band gap [6,27]. The performances of the photovoltaic devices in particular changes significantly at different annealing temperatures, such as the phase separation for the bulk-heterojunction formation, the evolution of the film morphology and the device efficiency.

This paper investigates the effect of the annealing process on the efficiency of P3HT/PCBM photovoltaic devices due to variations in the annealing conditions in different environments (vacuum, N_2, Ar are studied here) by RTA equipment, and comparing with the traditional annealing in air by hot-plates.

2. Experimental

Fig. 1 shows the schematic diagram of the bulk-heterojunction photovoltaic devices, and their energy band structure. The fabrication procedures, and the device characteristics, are measured using the following method. The glass substrate with patterned indium thin oxide (ITO) film is used for the substrate of the photovoltaic devices. The sheet resistance is 30 Ω/square, and the film thickness is 150 nm. The glass substrate is chemically cleaned according to the method based on successive baths of methanol and acetone, using ultrasonic signals for 10 min, and then is rinsed in deionised (DI) water. A PEDOT:PSS layer is then deposited by spin-coating on

* Corresponding author. Address: School of Electrical Engineering, College of Engineering, Korea University, 5-1, Anam-Dong, Seongbuk-Gu, Seoul 136-713, Republic of Korea. Tel.: +82 2 3290 1325; fax: +82 2 3290 3671.
E-mail address: bkju@korea.ac.kr (B.-K. Ju).

1567-1739/$ - see front matter © 2010 Elsevier B.V. All rights reserved.
doi:10.1016/j.cap.2010.02.023

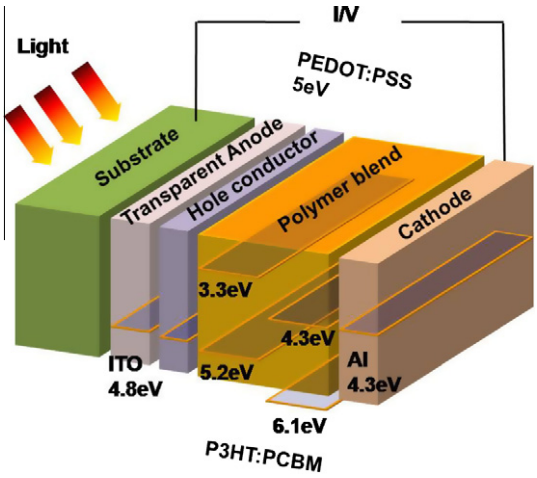

Fig. 1. Schematic diagram of the bulk-heterojunction photovoltaic devices, and their energy band structure.

the substrate. The device is then annealed using a hot-plate at 120 °C for 10 min in the air. The P3HT and PCBM have been purchased from Sigma–Aldrich Co. P3HT and PCBM are used as the electron donor and the electron acceptor, respectively. The solution is prepared with P3HT:PCBM 1:0.8 ratio, and is dissolved in a 22 mg/ml solution with chlorobenzene. The solution of the blend is homogenized for 4 h. The active layer is coated on the glass substrate by spin-coating at room temperature. The thickness of the deposited film is found to be about 160 nm. An aluminum contact electrode is deposited on the glass substrate through a shadow mask, by thermal evaporation (DOV Co., Ltd.), under a vacuum of 2×10^{-6} Torr, at room temperature. Finally, in order to analyze the effects of the annealing process of the organic photovoltaic devices, thermal annealing is carried out using thermal RTA equipment, at a temperature of 150 °C for 10 min in an different environments of vacuum, nitrogen, and argon, individually. For comparison purposes, basic photovoltaic devices are also produced; these are annealed on a hot-plate at a temperature of 150 °C for 10 min in air. The devices have active areas of 9 mm^2 and their current density versus voltage (*J–V*) measurements were performed, which was determined using a Keithley model 2400 source measuring unit. A class-A solar simulator with a 150 W Xenon lamp (Newport) served as a light source, where its light intensity was adjusted using a NREL-calibrated mono Si solar cell, with a KG-2 filter, for approximately AM 1.5 G1 sun light intensity. A UV/visible spectrophotometer (Lambda 35, PerkinElmer) is used to study the absorption spectra of the P3HT:PCBM films on the PEDOT:PSS coated ITO glass substrate. The surface morphology of the active layer is measured using an atomic force microscope (AFM, XE-100, Park Systems) in the trapping mode. External quantum efficiency (EQE) was measured as a function of wavelength from 300 to 800 nm using incident photo-to-current conversion equipment (IPCE) (PV measurements Inc.). Calibration was performed using a silicon photodiode G425, which was NIST-calibrated as a standard. The crystalline structure of the organic photovoltaic films was analyzed using two-dimensional X-ray Diffraction (XRD, D/max 2200 V) spectroscopy.

3. Results and discussion

Fig. 2 shows the AFM image of the surface morphology of the photovoltaic devices annealed by hot-plate in air, and the devices annealed using RTA equipment at a temperature of 150 °C for 10 min in environments of a vacuum, nitrogen, and argon, individually. The root mean square (RMS) roughnesses are 2.45 nm, 2.86 nm, 3.11 nm and 3.50 nm for annealing in vacuum, nitrogen, argon, and hot-plate for the P3HT:PCBM thin-films, respectively. The surface of the spin-coated organic film is both homogeneous and smooth. However, after annealed devices in vacuum, the surface morphology is smoother than others. In previously reported studies relating to morphology, a rough surface was mentioned as the self-organization signature of polymers. Thus, surface morphology has been reported that the organic photovoltaic devices

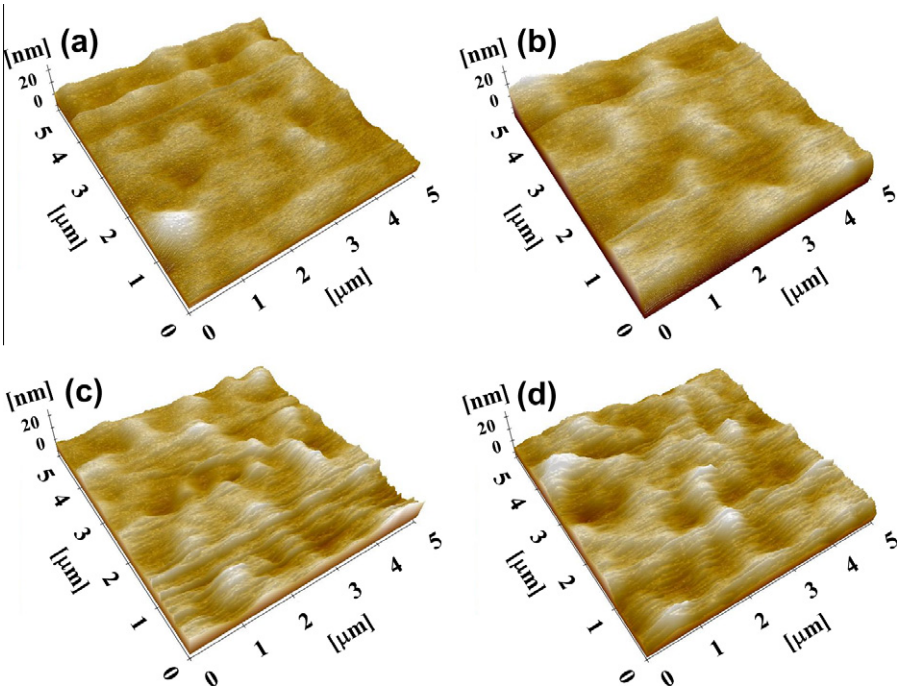

Fig. 2. The AFM image of the surface morphology of the photovoltaic devices annealed using RAT equipment at temperature of 150 °C for 10 min in (a) a vacuum, (b) nitrogen, (c) argon, and (d) the photovoltaic devices annealed by a hot-plate in air.

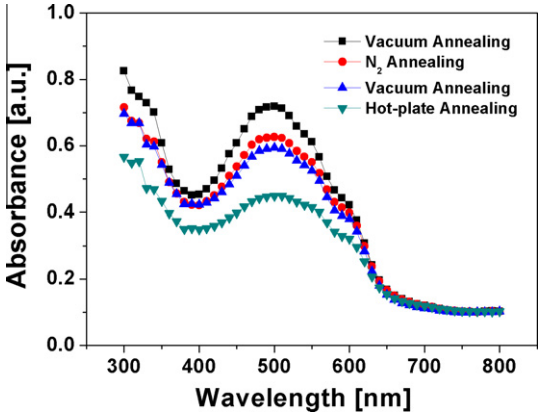

Fig. 3. UV/visible absorption spectra of annealed photovoltaic devices from the different annealing environments. The thermal annealing condition of photovoltaic devices is annealed using RAT equipment at a temperature of 150 °C for 10 min in different environments (vacuum, nitrogen, and argon, individually). The basic photovoltaic device was annealed on a hot-plate at 150 °C for 10 min in air.

are characterized high electrical performance on the smooth surface rather than on the rough surface [3,20].

Fig. 3 shows the UV/visible absorption spectra of the annealed photovoltaic devices, from the different annealing environments. The spectrum of the photovoltaic devices annealed by the RTA equipment shows one broad peak at 500 nm as a contribution of the polymer, and one at 320 nm due to the absorption of the PCBM. With respect to pristine P3HT, the absorption peak of the annealed photovoltaic devices is blue-shifted, and the whole spectrum is less structured due to the presence of the PCBM, which strongly limits the self-organizing property of P3HT. Generally, the crystalline structure and strong interchain interaction of P3HT could be obtained using high boiling point solvent and large enough solvent evaporation time [20]. However, as shown in Fig. 3, the absorption spectrum peaks of the photovoltaic devices from the various gas annealed environments are higher for annealed device in vacuum than for annealed devices in N_2, Ar and hot-plate and the photovoltaic device annealed by the hot-plate shows the lowest absorption rate. This tendency also depends on thermal annealing conditions. The interpenetrating networks and uniform distributions of P3HT:PCBM profitable for charge generation and transportation, are shown clearly in the AFM images of Fig. 2 for annealed device in vacuum than for annealed devices in N_2, Ar and hot-plate. It demonstrates that thermal annealing conditions as corresponding to slower evaporation of solvent, result in the higher degree of crystallinity and longer conjugation length of P3HT [28,29]. The shift of π–π^* transition absorption peaks to higher energy indicates an increasing density of conformational defects, equivalent to non-planarity, and causes loss of conjugation [28,29]. Therefore, it is confirmed slow evaporation of solvent with annealing conditions leads to higher degree of polymer ordering which is efficient for carrier generation and transportation. Especially, the reaction related between films of organic photovoltaic cell and gases such as N_2 and Ar is unclear.

Fig. 4a shows the *J*–*V* characteristics of annealed photovoltaic devices from different annealing ambients. The photovoltaic devices are measured with the *J*–*V* curve tracer with solar simulator, under AM 1.5G (100 mW/cm^2) irradiation intensity, in air. With the photovoltaic device annealed in a vacuum using the RTA equipment, the highest short-circuit current density (J_{sc}) is obtained (=8.74 mA/cm^2) and the device annealed by the hot-plate shows the lowest J_{sc}. Therefore, it is concluded that the decreased J_{sc} is due to the reduced degree of P3HT crystallinity, as shown in the absorption intensity of the active layer, and in the surface morphology. As a result, although these values are lower than

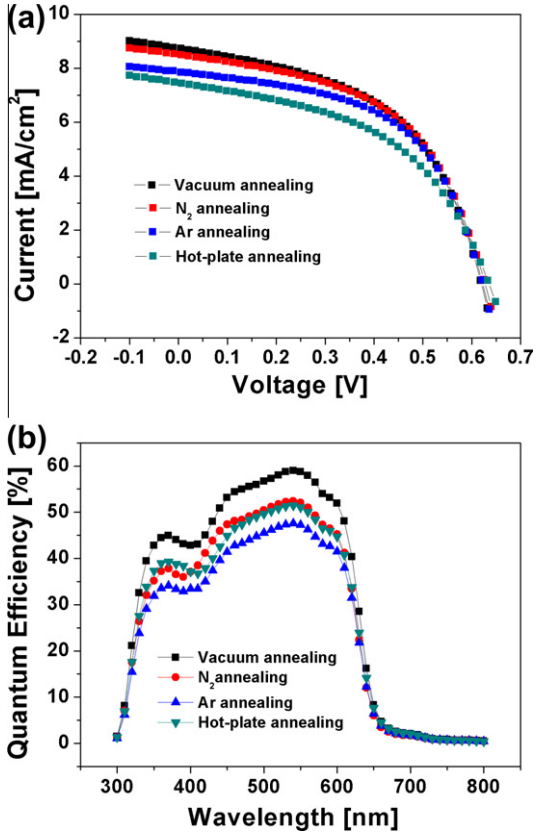

Fig. 4. (a) The current density–voltage (*J*–*V*) characteristics of annealed photovoltaic devices from the different annealing conditions and (b) the measured external quantum efficiency (EQE) of the organic photovoltaic devices using the incident photo-to-current conversion equipment (IPCE).

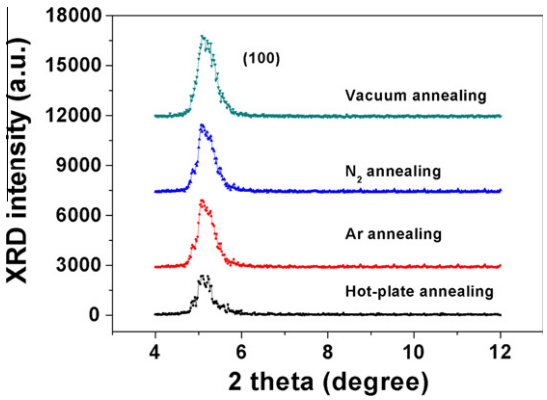

Fig. 5. The XRD patterns of the photovoltaic devices annealed in vacuum, N_2, Ar, and hot-plate.

previously reported ones [7], this observation shows the clear tendency of the photovoltaic device performances to be dependent on the thermal annealing conditions. It is expected that J_{sc} and the efficiencies can be improved by fabricating the photovoltaic devices under inert gas conditions [30].

Fig. 4b shows the IPCE spectra for the same films as in Fig. 4a. It can be seen that the J_{sc} for the photovoltaic devices are greatly increased by extending the annealing time to 10 min in vacuum conditions. The effect on the J_{sc} is clearly observed from the EQE spectra, which, in contrast, shows an increase over the entire

Table 1
The electrical characteristics of the annealed photovoltaic devices, from the different annealing environments.

	Annealing ambient	RMS roughnesses (nm)	V_{OC} (V)	J_{SC} (mA/cm^2)	*FF* (fill-fact)	E_{ff} (%)
Sample 1	Vacuum	2.45	0.62	8.74	51.06	2.77
Sample 2	N_2	2.86	0.63	8.51	51.64	2.76
Sample 3	Ar	3.11	0.62	7.86	53.96	2.64
Sample 4	Hot-plate (air)	3.50	0.63	7.45	48.36	2.29

wavelength range for the annealing conditions. This result shows that the trend of EQE as a function of the annealing conditions is coincident with the current density of the organic photovoltaic devices.

Fig. 5 shows the XRD patterns of the photovoltaic devices annealed in vacuum, N_2, Ar, and hot-plate, respectively. The XRD patterns strongly support the results mentioned for the different annealing environments. The intensity of P3HT is higher for the vacuum annealed device, and it gradually decreases for annealed devices in N_2, Ar and hot-plate, respectively. It again verifies that the crystallinity of P3HT improved after annealing in vacuum environment due to slow evaporation of the solvent as shown in AFM image of Fig. 2. Therefore, we demonstrated crystalline polymer structure and well-ordered polymer chains by slow evaporation of the solvent with vacuum annealing through the XRD analysis. For a comparison of the electrical characteristics for the annealing environments, the important parameters for all the fabricated devices are summarized in Table 1. Here, an open circuit voltage (V_{oc}) is slightly changed, in accordance with the annealing conditions of the photovoltaic devices where V_{oc} affects the energetic relationship between the highest occupied molecular orbital (HOMO) of the donor and the lowest unoccupied molecular orbital (LUMO) of the acceptor [31]. This seems to explain the results of the reduced V_{oc}, which originated because of the reduction in the effective bandgap as the interchain interactions and the chain lengths are increased [32]. The photovoltaic devices annealed by RTA equipment in vacuum show the highest absorption rate, J_{sc} and E_{ff}, respectively. Therefore, the V_{oc} of the devices annealed in the vacuum conditions are slightly decreased. The *J–V* characteristics results are in accordance with the absorption spectra, as shown in Fig. 3. Thus, the photo-current–voltage characteristics from the photovoltaic devices annealed in a vacuum have shown V_{oc} of 0.62 V, I_{sc} of 8.74 mA/cm^2, and E_{ff} of 2.77%. The device efficiency increased from 2.29% (hot-plate annealing) to 2.77%, after annealing at a temperature of 150 °C for 10 min in a vacuum. As a result, the organic photovoltaic devices annealed in a vacuum show significantly enhanced efficiencies compared with those annealed in different gaseous environments.

4. Conclusions

The effects of the annealing process on the performance of P3HT/PCBM photovoltaic devices have been studied in terms of the resulting efficiencies. In order to analyze the effects of the annealing processes for producing organic photovoltaic devices, the devices have been annealed using thermal RTA equipment, at a temperature of 150 °C for 10 min in different environments of a vacuum, nitrogen, and argon, individually. The basic photovoltaic devices have been annealed on a hot-plate, at a temperature of 150 °C for 10 min in air. As can be seen from the results of the UV/visible spectroscopy, J_{sc} and E_{ff}, the photovoltaic devices annealed by the hot-plate have shown the lowest efficiencies, whereas the performances of the devices annealed in a vacuum by RTA equipment, show the highest efficiencies. The photo–current–voltage characteristics, from the photovoltaic device annealed in a vacuum have shown V_{oc} of 0.62 V, I_{sc} of 8.74 mA/cm^2, and E_{ff} of 2.77%. The device efficiency has been seen to increase from 2.29% (for hot-plate annealing) to 2.77% after annealing at a temperature of 150 °C for 10 min in a vacuum. Thus, the organic photovoltaic devices annealed in a vacuum have significantly enhanced efficiencies compared with those annealed in different gaseous environments.

Acknowledgements

This work was supported by the IT R&D Program of MKE/KEIT (No. 2009-F-016-01, Development of Eco-Emotional OLED Flat-Panel Lighting), the IT R&D Program (No. 2008-F-024-02, Development of Mobile Flexible IOP Platform) of MKE in Korea, the ERC program of the Korea Science and Engineering Foundation (KOSEF) grant funded by the Korea Ministry of Education, Science and Technology (MEST), (No. R11-2007-045-01003-0), and the National Research Laboratory (NRL, No. R0A-2007-000-20111-0) Program.

References

[1] G. Fanchini, S. Miller, B.B. Parekh, M. Chhowlla, Nano Lett. 8 (2008) 2176–2179.
[2] S.H. Park, A. Roy, S. Beaupre, S. Cho, N. Coates, J.S. Moon, D. Moses, M. Leclerc, K. Lee, A.J. Heeger, Nat. Photon. 3 (2009) 297–302.
[3] C.N. Hoth, P. Schilinsky, S.A. Choulis, C.J. Brabec, Nano Lett. 8 (2008) 2806–2813.
[4] W.Y. Wong, J. Organomet. Chem. 634 (2009) 2644–2647.
[5] C.J. Yang, T.Y. Cho, C.L. Lin, C.C. Wu, Appl. Phys. Lett. 90 (2007) 173507.
[6] C. Zhang, S.W. Tong, C. Jiang, E.T. Kang, D.S.H. Chan, C. Zhu, Appl. Phys. Lett. 93 (2008) 043307.
[7] J.Y. Kim, K. Lee, N.E. Coaters, D. Moses, T.Q. Nguyen, M. Dante, A.J. Heeger, Science 317 (2007) 222.
[8] S. Bertho, G. Janssen, T.J. Gleij, B. Conings, W. Moons, A. Gadisa, J. D'Haen, E. Goovaerts, L. Lutsen, J. Manca, D. Vanderzande, Sol. Energy Mater. Sol. Cells 92 (2008) 753–760.
[9] M.H. Petersen, Ol Hagemann, K.T. Nielsen, M. Jorgensen, F.C. Krebs, Sol. Energy Mater. Sol. Cells 91 (2007) 996–1009.
[10] C. Lungenschmied, G. Dennler, H. Neugebauer, S.N. Sariciftci, M. Glatthaar, T. Meyer, A. Meyer, Sol. Energy Mater. Sol. Cells 91 (2007) 379–384.
[11] M. Niggemann, B. Zimmermann, J. Haschke, M. Glatthaar, A. Gombert, Thin Solid Films 516 (2008) 7181–7187.
[12] R. Franke, B. Maennig, A. Petrich, M. Pfeiffer, Sol. Energy Mater. Sol. Cells 92 (2008) 732–735.
[13] M. Jorgensen, K. Norrman, F.C. Krebs, Sol. Energy Mater. Sol. Cells 92 (2008) 686–714.
[14] J.Y. Lee, S.T. Connor, Y. Cui, P. Peumans, Nano Lett. 8 (2008) 689–692.
[15] Y.F. Lim, S. Lee, D.J. Herman, M.T. Lloyd, J.E. Anthony, Appl. Phys. Lett. 93 (2008) 193301.
[16] Y. Kim, A.M. Ballantyne, J. Nelson, D.D.C. Bradley, Org. Electron. 10 (2009) 205–209.
[17] T. Taima, J. Sakai, T. Yamanari, K. Saito, Sol. Energy Mater. Sol. Cells 93 (2009) 742–745.
[18] L.L. Kazmerski, J. Eletron. Spectroscopy Related Phenomena 150 (2006) 105–135.
[19] T. Yamanari, T. Taima, K. Hara, K. Saito, J. Photochem. Photobiol. Chem. 182 (2006) 269–272.
[20] W.H. Baek, H. Yang, T.S. Yoon, C.J. Kang, H.H. Lee, Y.S. Kim, Sol. Energy Mater. Sol. Cells 93 (2009) 1263–1267.
[21] Y.K. Kim, S.A. Choulis, J. Nelson, D.D.C. Bradley, S. Cook, J.R. Durrant, Appl. Phys. Lett. 86 (2005) 063502.
[22] J. Sakai, T. Taima, T. Yamanari, K. Saito, Sol. Energy Mater. Sol. Cells 93 (2009) 1149–1153.
[23] M. Reyes-Reyes, K. Kim, D.L. Carrol, Appl. Phys. Lett. 87 (2005) 083506.
[24] F. Padinger, R.S. Rittberger, N.S. Sariciftci, Adv. Funct. Mater. 13 (2003) 85–88.
[25] Q. Wei, T. Nishizawa, K. Tajima, K. Hashimoto, Adv. Mater. 20 (2008) 2211–2216.
[26] S.S. Kim, S.I. Na, J. Jo, D.Y. Kim, Y.C. Nah, Appl. Phys. Lett. 93 (2008) 073307.
[27] D.W. Zhao, X.W. Sun, C.Y. Jiang, A.K.K. Kyaw, G.Q. Lo, D.L. Kwong, Appl. Phys. Lett. 93 (2008) 083305.

[28] S. Hotta, S.D.D.V. Rughooputh, A.J. Heeger, Conducting polymer composites of soluble polythiophenes in polystyrene, Synth. Met. 22 (1987) 79–87.
[29] O. Inganas, W.R. Salaneck, J.E. Osterholm, J. Laakso, Thermochromic and solvatochromic effects in poly(3-hexylthiophene), Synth. Met. 22 (1988) 395–406.
[30] Y. Kim, S.A. Choulis, J. Nelson, D.D.C. Bradley, Appl. Phys. Lett. 86 (2005) 063502.
[31] B. C Thomson, J.M.J. Frechet, Chem. Int. Ed. 47 (2008) 58–77.
[32] J. Cornil, D. Beljonne, J.P. Calbert, J.L. Bredas, Adv. Mater. 13 (2001) 1053–1067.